Research Article

Journal of Environmental Nanotechnology

Hydrothermal Synthesis and Characterization of Tin Oxide Nanoparticles

T. Regin Das[1], M. Meena[2*], I. Vetha Potheher[3], P. Aji Udhaya[4]

[1]Department of Physics, Lekshmipuram Arts and Science College, Neyyoor, Nagarcoil, Tirunelveli, TN, India
[2]Department of Physics, S.T. Hindu College, Nagercoil, Abishekapatti, Tirunelveli, TN, India
[3]Department of Physics, Bharathidasan Institute of Technology, Anna University, BIT Campus, Tirchy, TN, India
[4]Department of Physics, Holy Cross College, Nagercoil, Abishekapatti, Tirunelveli, TN, India
Received: 12.01.2020 Accepted: 22.02.2020 Published: 30-06-2020
*meenataj19@gmail.com

ABSTRACT

Metal oxide nanoparticles have potential applications in a wide range of fields like medicine and environmental science. Tin oxide (SnO_2) has been applied as a semiconductor nanomaterial in electronics. Tin oxide is a widely used and intensively studied n-type semiconductor. The research on tin oxide semiconductors has been growing due to the wide range of applications, especially as photo sensors, catalysts and antistatic coating. The electrical conductivity and luminescence properties of SnO_2 are mainly decided by the oxygen vacancy present in it. This work was intended to synthesize Tin oxide (SnO_2) nanoparticles via a one-step hydrothermal method and study the effect of annealing temperature on its properties. As prepared samples were annealed at two different temperatures and the samples were characterized by Powder X-Ray Diffraction (PXRD), Ultraviolet Diffusion Reflectance Spectroscopy (UV-DRS) and Photo Luminescence (PL). The dependence of structural and optical properties with temperature was discussed.

Keywords: Oxide; Annealing temperature; PXRD; UV-DRS; PL.

1. INTRODUCTION

Nanoparticle plays a significant role in research and development of the device, systems and structures in numerous areas. Tin oxide is one of the most important materials due to its high degree of transparency in the visible spectrum, strong physical and chemical interaction with adsorbed species, low operating temperature, and strong thermal stability in the air up to 500 °C. Tin oxide (SnO_2) is classified as a II-VI composite semiconductor, based on its group II and VI periodic table components with 3.60 eV and 3.75 eV direct and indirect energy band gaps (Jain and Kumar, 2004). SnO_2 nanoparticle preparation can be achieved using various techniques, including co-precipitation (Arularasu *et al.* 2018) sol-gel (Gu *et al.* 2004), solvothermal decomposition (Davar *et al.* 2010), microwave hydrothermal synthesis (Ponzoni *et al.* 2015), and precipitation (Gaber *et al.* 2014) techniques. However, issues related to the complexity of the synthetic process include the creation of a pure by-product, reagent toxicity and longer reaction times, which have made industrial SnO_2 nanoparticle generation highly challenging to achieve (Tran *et al.* 2017).

It is essential to have inexpensive methods for obtaining nanoparticles with no special atmosphere and high temperature. The hydrothermal method is a suitable chemical method in nanoparticle synthesis because it does not require high pressure and high temperature, and impurities are removed by filtration and washing. Tin is present in two oxidation states; therefore, two types of oxides are possible: Stannous oxide (SnO-romarchite) and Stannic oxide (SnO_2- cassiterite) (Vila and Rodiguez – Paez, 2009). SnO_2 is an n-type semiconductor and is more stable than SnO. It is widely used in optoelectronic devices (He *et al.* 2006), electrodes for Lithium-ion batteries (He *et al.* 2005), solar cells (Ge *et al.* 2006), transistors, and gas sensors to detect combustible gases such as H_2S, CO, Liquid petroleum, NO_2 and C_2H_5OH (Hwang and Choi, 2009).

The surface-to-volume ratio (S/V) of SnO_2 nanoparticles is high compared to the bulk tin oxide, which results in increased sensitivity and adsorption. The electrical conductivity and luminescence properties of SnO_2 are mainly decided by the oxygen vacancy present in SnO_2 lattice (Gu *and* Wang, 2004), and they are also affected by surface to volume (S/V) ratio. In this report, the particle size and lattice parameters were analyzed using XRD for SnO_2 nanoparticles; bandgap and photoluminescence were measured using UV and PL studies for unannealed SnO_2 and SnO_2 annealed at100 °C and 600 °C.

2. EXPERIMENTAL PROCEDURE

The materials used for the preparation of SnO_2 nanoparticles were dihydrated Stannous chloride ($SnCl_2.2H_2O$), urea (CH_4N_2O) and Sodium hydroxide (NaOH) pellets. The calculated amount of stannous chloride was dissolved in 100 ml of pure distilled water as the starting solution. The calculated amount of urea solution was also prepared separately by dissolving urea in 100 ml of distilled water. Then, the solutions were mixed and stirred well for about 15 minutes, during which NaOH solution was added drop-by-drop such that it attains a suitable pH value. The resultant solution is then stirred for 15 minutes using magnetic stirrer. The light milky colored solution obtained was then changed to Borosil pot and placed in a microwave oven. The oven was operated for 30 minutes at medium temperature.

After cooling, the product obtained was then washed with distilled water and benzene. Then, it was filtered using Wattman filter paper and dried at room temperature. Parts of the prepared samples were then annealed at 100 °C and 600 °C for two hours in the heating furnace.

The structural behavior of as-prepared and annealed SnO_2 was characterized by XRD analysis with X-ray wavelength of 1.5406 A° and scanning range of 3 to 80 degrees. The mean crystallite size (D) of the nanoparticles were estimated using the Debye-Scherrer formula,

$$D = 0.9\lambda / \beta \cos\theta$$

where, λ, β, and θ are the X-ray wavelength (1.5406A°), full-width half-maximum (FWHM) of diffraction peak and diffraction angle, respectively. Bradley-Joy and Nelson - Rilay graphs were also drawn for the samples to get the corrected value of the lattice parameters.

3. RESULT AND DISCUSSION

3.1 X-ray Diffraction Analysis

All the synthesized samples were characterized for their crystal structure, particle size, and lattice parameters. The XRD pattern of prepared SnO_2 has been given in Fig. 1. It shows a crystalline phase with broad diffraction peaks corresponding to a tetragonal structure. All the peaks of the XRD belonging to the tetragonal lattice of SnO_2 were coinciding with the tetragonal structure of SnO_2 in JCPDS file (File No.: 88-0287). The lattice parameters were calculated using unit cell software (Method of TJB Holland & SAT Redform 1995).

The spacing between diffracting planes (d) of SnO_2 was calculated by Bragg's equation,

$$2d \sin\theta = n\lambda$$

The lattice parameters (a=b≠c) for tetragonal phase structure were determined by the equation,

$$1/d = (h^2 + k^2)/a^2 + l^2/c^2$$

The calculated values of a, b and c and cell volumes have been given in Table 1. The increase of annealing temperature from 100 to 600 °C shows no significant variation in the lattice parameters and cell volume, due to the dehydroxylation of the material owing to the presence of some hydroxyl group in the Tin oxide crystallites annealed at 100 °C, which generated a non-perfect rutile structure. The samples annealed at higher temperatures showed the perfect rutile structure (Antonio *et al.* 2003). The narrowness of the peaks towards the increased annealing temperature indicated that SnO_2 nanoparticles crystallize with the increase in temperature.

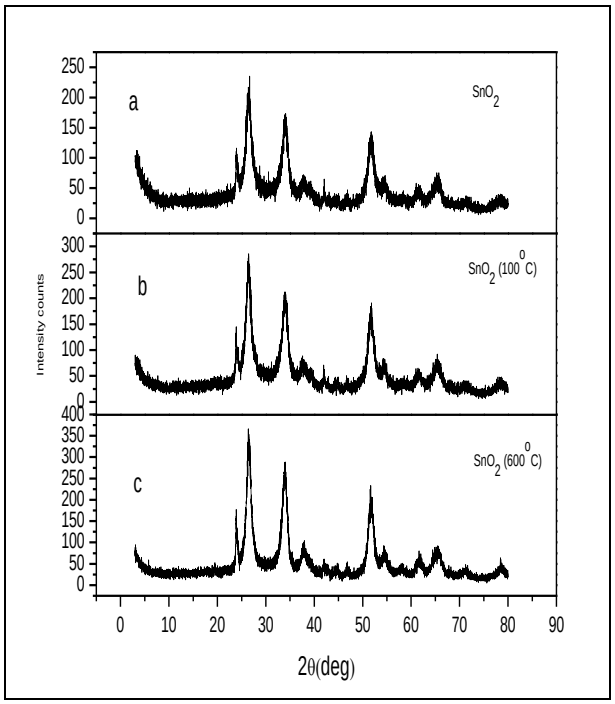

Fig. 1: XRD patterns of SnO_2: (a) un-annealed (b) annealed at 100 °C and (c) annealed at 600 °C.

The crystallite sizes of SnO_2 nanoparticles measured using the Scherrer formula were 5.17, 6.32 and 6.43 nm for unannealed SnO_2, annealed at 100 °C and annealed at 600 °C, respectively. Fig. 2 is the Williamson-Hall plot drawn between 4 sinθ and β cosθ. The intercept of β cosθ value at y-axis gives 0.9 λ/D from which the particle size D was calculated; the slope of the line indicated the lattice strain (C_ϵ).

Table 1. Cell parameters and Cell volume of SnO_2

Sample	a	c	Cell Volume
SnO_2-unannealed	4.76	3.17	71.97
SnO_2-annealed at 100 °C	4.77	3.17	72.12
SnO_2-annealed at 600 °C	4.76	3.19	72.29

From Tables 1 and 2, it was observed that the strain value decreased and particle size increased as the annealing temperature increased.

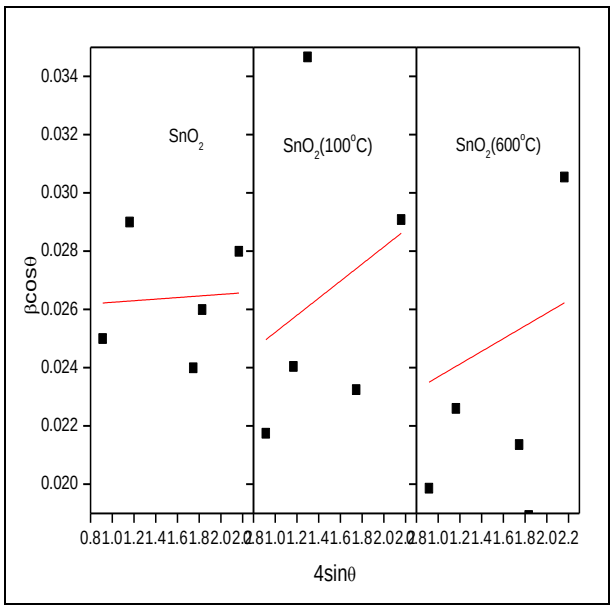

Fig. 2: Williamson-Hall plot of SnO_2 annealed at different temperatures.

Table 2. The Intercept and Slope of Williamson-Hall plot for SnO_2.

Sample	Unannealed SnO_2	SnO_2 - annealed at 100 °C	SnO_2 - annealed at 600 °C
Intercept	0.019	0.022	0.020
Slope (strain)	0.006	0.003	0.002
Particle size (nm)	5.17	6.32	6.43

3.2 UV-DRS Analysis

In order to study the effect of annealing on the optical properties of SnO_2 nanoparticles, UV-diffuse reflectance measurements were carried out. Fig. 3 shows the recorded UV spectra of the prepared unannealed samples and samples annealed at 100 °C and 600 °C.

The diffuse reflectance spectra studies are more important to estimate the optical bandgap of the materials. The calculated band gaps for unannealed SnO_2 nanoparticles and particles annealed at 100 °C and 600 °C were found to be 3.744, 3.60 and 3.21 eV, respectively. Our current study has shown that as the annealing temperature increased, the bandgap energy decreased. It was suggested that the decrease in bandgap could be due to transitions between Sn^{2+} ion d-shell electrons' valance and conduction bands (Choi et al. 1996). Given this, it is difficult to eradicate the particle size effect on the bandgap.

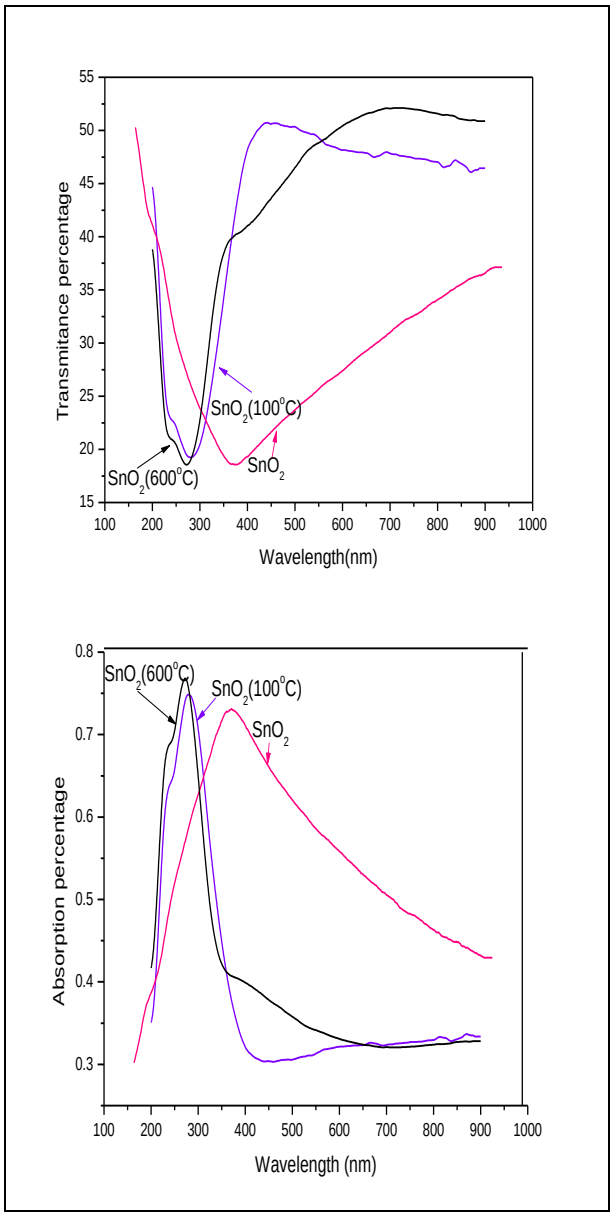

Fig. 3: Absorption and transmittance spectra of SnO_2 annealed at different temperatures.

It is possible to change the band structure and material attributes due to the reduction in the particle size

with a reduction in the bandgap. Thus, smaller particle sizes can be associated with overlap with s-electron and p-electron conduction bands separating in higher energy conditions. Higher calcination temperatures were associated with lower bandgap values. It was suggested that the temperature rise may cause an increase in the absorption coefficient because of an increase of defected states. Electron-hole pairs are produced through photon absorption, generating a field that could change the optical attributes and electronic structure of nanoparticle products.

3.3 Photoluminescence Study

Besides the size quantization, surface effects are also known to influence the optical properties of the nanometer particles. It has been shown recently that the photoluminescence emission of the nanocrystals is sensitive to the presence of defects that might arise because not all the dangling bonds on the particle surface can be saturated by molecular legends (Yang *et al*. 1996).

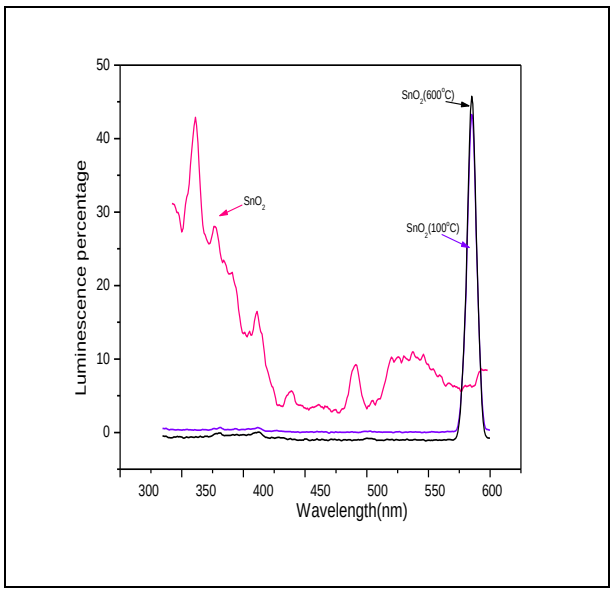

Fig. 4: Photoluminescence spectra of SnO_2 nanoparticles annealed at different temperatures.

In the present study, photoluminescence emission spectra were recorded in the wavelength range of 300 to 600 nm for the excitation at 585 nm. Fig. 4 shows the recorded photoluminescence spectra of SnO_2 nanoparticles annealed at various temperatures.

4. CONCLUSION

The results of this study have demonstrated the effect of annealing on particle size. The nanoparticles were synthesized without the requirement of any special atmosphere and pressure. This study provides an inexpensive and easy method to prepare and improve the quality of SnO_2 nanoparticles. Lesser particle sizes were obtained at lower annealing temperatures. The optical studies have shown that band gap variation can also be achieved by varying the annealing temperature corresponding to the particle size.

FUNDING

This research received no specific grant from any funding agency in the public, commercial, or not-for-profit sectors.

CONFLICTS OF INTEREST

The authors declare that there is no conflict of interest.

REFERENCES

Arularasu, M., Anbarasu, M., Poovaragan, S., Sundaram, R., Kanimozhi, K., Magdalae, C. M., Kaviyarasu, K., Thema, F. T., Letsholathebe, D., Mola, G. T. and Maaza, M., *J. Nanosci. Nanotechnol*., 18(5), 3511–3517 (2018). https://dx.doi.org/10.1166/jnn.2018.14658

Choi, W. K., Jung, H. J. and Koh, S. K., Chemical shifts and optical properties of tin oxide films grown by a reactive ion assisted deposition, *J. Vac. Sci. Technol. A.*,14, 359–366 (1996). https://dx.doi.org/10.1116/1.579901

Davar, F., Salavati-Niasari, M. and Fereshteh, Z., Synthesis and characterization of SnO_2 nanoparticles by thermal decomposition of new inorganic precursor, *J. Alloys Compd*., 496(1-2), 638–643 (2010). https://dx.doi.org/10.1016/j.jallcom.2010.02.152

Ge, J. P., Wang, J., Zhang, H. X., Wang, X., Peng, Q. and Li, Y.D., High ethanol sensitive SnO_2 microspheres, *Sens. Actuators. B:Chem*., 113(2), 937-943 (2006). https://dx.doi.org/10.1016/j.snb.2005.04.001

Gu, F., Wang, S. F., Lu, M. K., Zhou, G. J., Xu, D. and Yuan, D. R., Photoluminescence properties of SnO_2 nanoparticles synthesized by sol-gel method, *J. Phys. Chem.* B., 108, 8119-8123 (2004). https://dx.doi.org/10.1021/jp036741e

Gu, F., Wang, S. F., Lü, M. K., Zhou, G. J., Xu, D. and Yuan, D. R., Photoluminenescence properties of SnO_2 nanoparticles synthesized by sol-gel method, *J. Phys. Chem. B.*, 108, 8119–8123 (2004). https://dx.doi.org/10.1021/jp036741e

He, Jr. H., Wu, Te. H., Hsin, C. L., Li, K. M., Chen, L. J., Chueh, Y. L. and Wand, Z. L., Beaklike SnO_2 nanorods with strong photoluminescent and field-emission properties, *Small*, 2(1), 116-120 (2005). https://dx.doi.org/10.1002/smll.200500210

He, Z. Q., Li, X. H., Xion, L. Z., Wu, X. M., Xiao, Z. B. and Ma, M. Y., Wet chemical synthesis of tin oxide-based material for lithium ion battery anodes, *Mater. Res. Bull*., 40(5), 861-868 (2005). https://dx.doi.org/10.1016/j.materresbull.2004.06.021

Hwang, I. S., Choi, J. K., Kim, S. J., Dong, K. Y., Kwon, J. H., Ju, B. K. and Lee, H. J., Enhanced H_2S sensing characteristics of SnO_2 nanowires functionalized with CuO, *Sens. Actuators. B: Chem.*, 142(1), 105-110 (2009). https://dx.doi.org/10.1016/j.snb.2009.07.052

Jain, G. and Kumar, R., Electrical and optical properties of tin oxide and antimony doped tin oxide films, *Opt. Mater*., 26(1), 27–31 (2004). https://dx.doi.org/10.1016/j.optmat.2003.12.006

Ponzoni, C., Cannio, M., Boccaccini, D., Bahl, C. R, H., Agersted, K. and Leonelli, C. S., Ultrafast microwave hydrothermal synthesis and characterization of $Bi1\text{-}xLaxFeO_3$ micronized particles, *Mater. Chem. Phys.*, 162, 69–75 (2015). https://dx.doi.org/10.1016/j.matchemphys.2015.05.002

Tran, V.-H., Ambade, R. B., Ambade, S. B., Lee, S. H. and Lee, I. H., Low temperature solution – processed SnO_2 nanoparticles as a cathode buffer layer for inverted organic solar cells, *ACS Appl. Mater. Interfaces*., 9(2), 1645–1653 (2017). https://dx.doi.org/10.1021/acsami.6b10857